Available online at www.sciencedirect.com
ScienceDirect
Journal of Power Sources 160 (2006) 1349–1354
JOURNAL OF POWER SOURCES
www.elsevier.com/locate/jpowsour

Study of the charging process of a $LiCoO_2$-based Li-ion battery

S.S. Zhang *, K. Xu, T.R. Jow

U.S. Army Research Laboratory, AMSRD-ARL-SE-DC, Adelphi, MD 20783-1197, USA

Received 30 January 2006; received in revised form 14 February 2006; accepted 15 February 2006
Available online 18 April 2006

Abstract

A three-electrode Li-ion cell with metallic lithium as the reference electrode was designed to study the charging process of Li-ion cells. The cell was connected to three independent testing channels, of which two channels shared the same lithium reference to measure the potentials of anode and cathode, respectively. A graphite/$LiCoO_2$ cell with a C/A ratio, i.e., the reversible capacity ratio of the cathode to anode, of 0.985 was assembled and cycled using a normal constant-current/constant-voltage (CC/CV) charging procedure, during which the potentials of the anode and cathode were recorded. The results showed that lithium plating occurred under most of the charging conditions, especially at high currents and at low temperatures. Even in the region of CC charging, the potential of the graphite might drop below 0 V versus Li^+/Li. As a result, lithium plating and re-intercalating of the plated lithium into the graphite coexist, which resulted in a low charging capacity. When the current exceeded a certain level (0.4*C* in the present case), increasing the current could not shorten the charging time significantly, instead it aggravated lithium plating and prolonged the CV charging time. In addition, we found that lowering the battery temperature significantly aggravated lithium plating. At −20 °C, for example, the CC charging became impossible and lithium plating accompanied the entire charging process. For an improved charging performance, an optimized C/A ratio of 0.85–0.90 is proposed for the graphite/$LiCoO_2$ Li-ion cell. A high C/A ratio results in lithium plating onto the anode, while a low ratio results in overcharge of the cathode.
© 2006 Elsevier B.V. All rights reserved.

Keywords: Li-ion battery; Charging; $LiCoO_2$; High rate; Low temperature

1. Introduction

Li-ion batteries are the most suitable power supply for many portable electronic devices, such as cellular phones, digital cameras and notebooks, because of their high energy and power density [1–4]. Regarding operating safety and cycling stability, the $LiCoO_2$ cathode has overall advantages over other cathode materials such as $LiMn_2O_4$ and $LiNi_{1-x}Co_xO_2$ ($x = 0.1$–0.2). Therefore, most batteries in the current market are based on $LiCoO_2$ chemistry. In practical applications, Li-ion batteries are often assembled together with a safety protection circuitry into a "battery pack" (or called "battery module") to meet the specific requirements of the power and volumetric space of various electronic devices [5–8]. Such a battery pack usually requires a specific charger that is controlled by a microprocessor with a pre-programmed charging algorithm. Normally, the charger is programmed to charge the battery pack through two continuous steps of constant-current/constant-voltage (CC/CV) charging. Most of the chargers are designed to provide about a 3-h charging time, during which the battery is first charged to 4.2 V at ∼1*C* to reach 60–70% of the capacity and then charged at the top voltage to reach the rest of the capacity [9–11]. This general charging program is purely based on the cell voltage, with little consideration of the practical potentials of the anode and cathode. In fact, the potentials of the electrodes are greatly affected by the charging conditions such as the charging current and the ambient temperature, and by the cell design such as the electrode loading and the reversible capacity ratio of the cathode to the anode (hereafter called the C/A ratio). Beyond normal operating potentials, the Li-ion chemistry inside the battery will be damaged, which can result in a permanent loss in battery performance. For example, an over-potential on the anode during discharge could corrode the supporting copper foil, while an over-potential on the cathode during charge could degrade the crystallographic structure of the cathode and cause oxidative decomposition of the electrolytic solvents. Therefore, it is important to understand and control the potentials of both electrodes for prolonged cycling life of Li-ion batteries.

* Corresponding author. Tel.: +1 301 394 0981; fax: +1 301 394 0273.
E-mail address: szhang@arl.army.mil (S.S. Zhang).

0378-7753/$ – see front matter © 2006 Elsevier B.V. All rights reserved.
doi:10.1016/j.jpowsour.2006.02.087

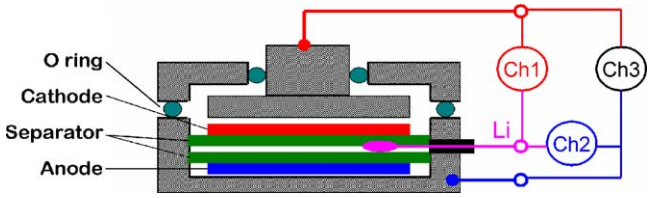

Fig. 1. A schematic of the testing cell and connection circuitry.

In this work, we focused on a graphite/$LiCoO_2$ chemistry to study the potential change of the anode and cathode, respectively, during the charging process. For this purpose, a three-electrode cell using metallic lithium as the reference electrode was designed to measure instantly the cell voltage and the potentials of the anode and cathode, respectively. We will discuss the effect of the charging current and ambient temperature on the potentials of the anode and cathode during the normal CC–CV charging and also will discuss the optimized C/A ratio for the design of a fast charging Li-ion cell.

2. Experimental

Electrode sheets of MCMB 25–28 anode (mesocarbon microbead with a 25 μm of averaged particle size and graphitized at 2800 °C) and $LiCoO_2$ cathode, supplied by a battery company, were cut into disks with a diameter of 1.75 in. (equal to an area of 15.5 cm^2) and dried at 110 °C under vacuum for 16 h before use. A 1.0 m $LiBF_4$ solution dissolved in a 1:1:3 (wt.) mixture of ethylene carbonate (EC), γ-butyrolactone (BL) and ethyl methyl carbonate (EMC) was used as the electrolyte. This solution has been proven to be an excellent low temperature electrolyte for many Li-ion batteries [12,13], and it has very good wetting capability for various types of Celgard® membranes.

In an argon-filled glove-box, a three-electrode Li-ion cell with metallic lithium as the reference electrode was assembled. The cell structure and connection circuitry for the tests are illustrated in Fig. 1, in which three independent testing channels were used to record the cell voltage (E_{cell}) and the potentials of the anode ($E_{(-)}$) and cathode ($E_{(+)}$), respectively. The lithium reference electrode, which was sandwiched between two Celgard® 2500 membranes and placed between the anode and cathode, was shared by Channel 1 and Channel 2 to measure the potentials of the $LiCoO_2$ cathode and MCMB anode, respectively. Channel 3 was connected to two ends of the cell to record the cell voltage. Before test, the cell was regularly formed by cycling at 0.1*C* twice and at 0.5*C* three times. In addition, similar three-electrode lithium cells with either the cathode or the graphite anode being replaced with a lithium foil were assembled to evaluate the reversible capacity of each electrode.

A Tenney Environmental Oven Series 942 was used to provide a constant-temperature environment for the test. A Maccor Series 4000 tester was employed to cycle the cell and to record the potentials of the cathode and anode by using the connection circuitry as shown in Fig. 1. For fair comparisons, all discharges were conducted at 12.5 mA (∼0.4*C*) and at 20 °C, and were ended at 2.5 V. For charging at low temperature, the oven temperature was stabilized for 6 h before charging to achieve thermal equilibrium of all the cell components. Using specified conditions (to be discussed later), the cell was charged to full capacity (4.2 V) by means of the CC–CV procedures. There was a 1-h rest between charging and discharging.

3. Results and discussion

3.1. The CC–CV charging profile

Fig. 2 exhibits a profile of the CC–CV charging, which has been used in most Li-ion battery chargers. This is shown in Fig. 2a where the cell is charged at a certain current to 4.2 V and then taper charged at 4.2 V. During CC charging, the cell voltage slowly climbs and the state-of-charge (SOC) of the cell linearly increases. After the voltage reaches the upper limit (4.2 V) at which the SOC reaches 71%, the charger controls the voltage constantly by reducing the current and the cell starts taper charging, to attain the remaining 29% SOC. For a Li-ion cell, the total charging time and its distribution between CC and CV steps are greatly affected by the charging conditions such as current and temperature. Generally, a larger ratio of the CC time to CV time favors a longer battery life, but it requires a longer charging time.

Fig. 2b shows a detailed correlation of E_{cell} with $E_{(-)}$ and $E_{(+)}$, which was recorded by the method shown in Fig. 1. Please note that in the whole charging process, there is a

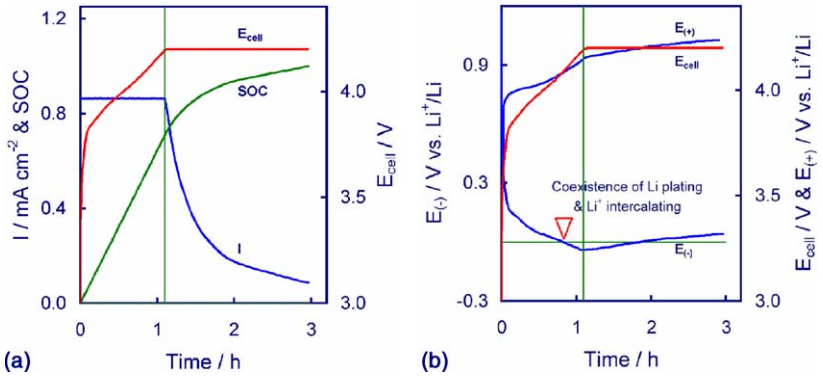

Fig. 2. Typical CC–CV charging profiles of a MCMB/$LiCoO_2$ Li-ion cell. (a) Cell voltage, current and SOC vs. charging time and (b) cell voltage, cathode potential and anode potential vs. charging time.

correlation below:

$$E_{\text{cell}} = E_{(+)} - E_{(-)} \quad (1)$$

Therefore, one channel, either Channel 1 or Channel 2 in Fig. 1, can be omitted by using Eq. (1). It is interesting to notice the change of the $E_{(-)}$ with the charging time. Starting with CC charging, the $E_{(-)}$ gradually declines and finally it becomes negative with respect to Li^+/Li reference, as indicated by a triangle in Fig. 2b. That is, lithium plating occurs in the late period of CC charging although graphite has not been fully lithiated. In other words, the following reactions may coexist on the graphite anode:

$$Li^+ - e \rightarrow Li_6 \quad (2)$$

$$\delta Li + Li_xC_6 \rightarrow Li_{x+\delta}C_6 \quad (3)$$

$$\delta Li^+ + Li_xC_6 - \delta e \rightarrow Li_{x+\delta}C_6 \quad (4)$$

As the plated lithium undergoes a subsequent reaction with Li_xC_6 to form $Li_{x+\delta}C_6$ (i.e., Eq. (3)), this could be very effective in suppressing the formation of dendritic lithium. Therefore, no short circuit was observed in the present work. Upon the start of CV charging, the $E_{(-)}$ slowly recovered to a normal level of the potential of graphite anode because of the decrease in current. During CV charging, the $E_{(+)}$ and $E_{(-)}$ are increased in parallel with an difference of 4.2 V.

3.2. The effect of the charging current

Correlations of the cell voltage and electrode potentials with charging time for different currents are compared in Fig. 3a–f, in which Fig. 3a with a slow charging rate (2.5 mA, equal to 0.08*C*) was used to measure the full capacity of the cell. It was determined that the cell has a capacity of 32.0 mAh. At the end of charging, the potentials of graphite and $LiCoO_2$ were 0.015

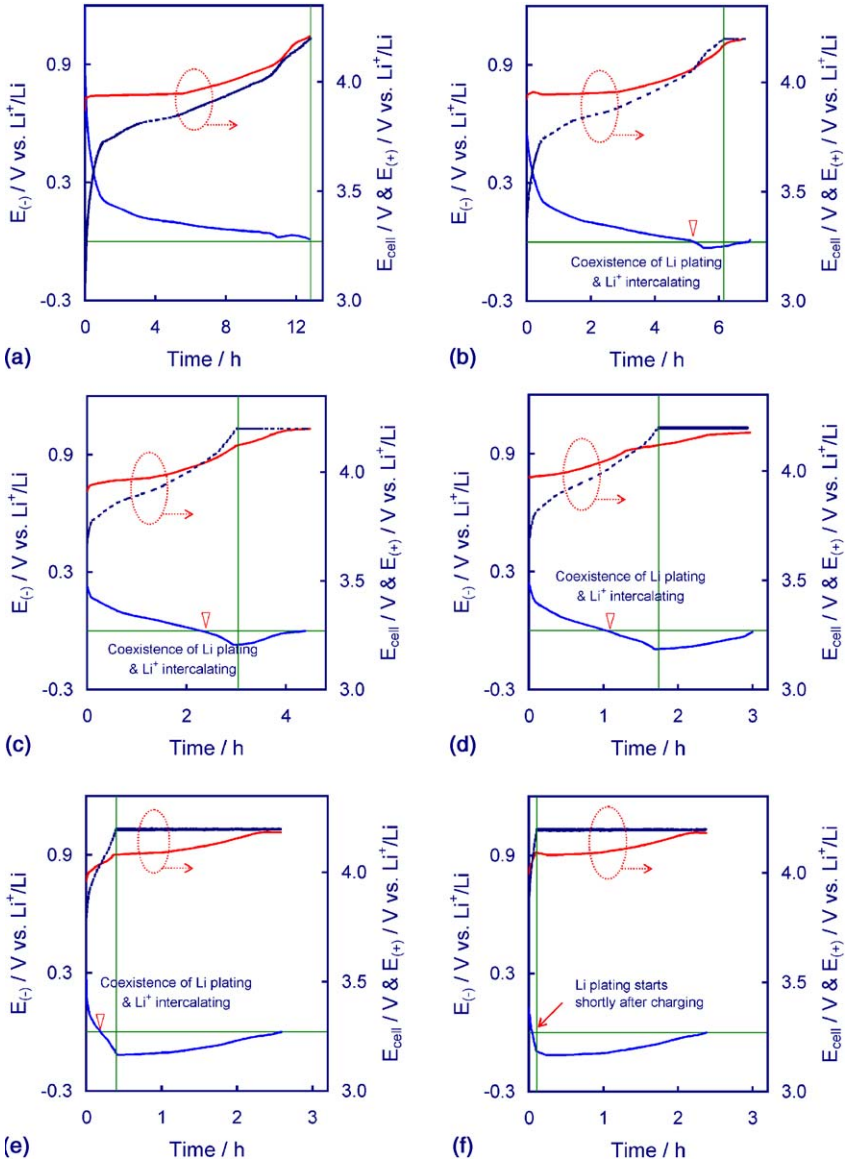

Fig. 3. Correlation of the cell voltage, cathode potential and anode potential with charging time for a 32 mAh MCMB/$LiCoO_2$ cell with different charging currents: (a) 2.5 mA, (b) 5 mA, (c) 8.3 mA, (d) 12.5 mA, (e) 25 mA and (f) 37.5 mA.

and 4.215 V versus Li^+/Li, respectively, and the cell voltage was 4.2 V. Lithium plating to different extents was observed at all the other currents (see Fig. 3b–f). A general trend is that lithium plating increases with the charging current, and that the plated lithium immediately starts to re-intercalate into graphite through a chemical reaction (Eq. (3)), as indicated by the fact that the $E_{(-)}$ slowly recovers to about 0 V versus Li^+/Li by the end of charging. It should be noted that the final $E_{(-)}$ is relatively low as compared with the normal potential of Li_xC_6 ($x = 1$). This is attributed to the over-potential caused by the small current at the end of charging (the final current was set to be 1.25 mA in the present experiments).

Charging time and its distribution between the CC and CV steps are summarized in Fig. 4, in which the charging capacities achieved by different currents also are plotted. It is shown that increasing the current does not shorten the charging time significantly, instead it greatly increases the portion of the CV time and reduces the charging effectiveness. As the current increases to 12.5 mA (0.4*C*) or higher, only 83–85% of the capacity can be charged although the same cut-off voltage and current are used. These results reveal that high charging currents are not appropriate for a Li-ion battery.

3.3. The effect of ambient temperature

The effect of temperature on the cell voltage and electrode potentials during charging at 5 mA is displayed in Fig. 5a–d.

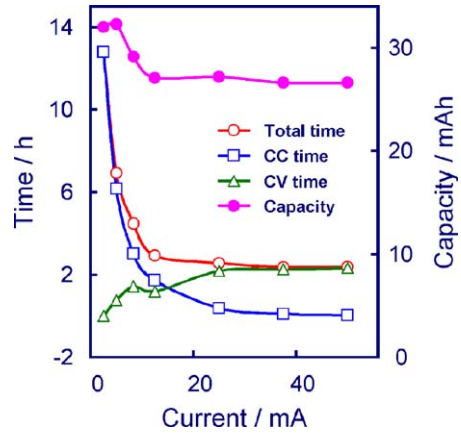

Fig. 4. Effect of charging currents on the distribution of CC and CV times and on the charging capacity for the MCMB/$LiCoO_2$ cell.

Similar to charging at high currents, lithium plating was observed in all the cases and it was aggravated by decreasing the temperature. In particular, the CC step vanishes as the temperature drops to −20 °C, where lithium plating occurs as soon as the charging starts and accompanies the whole charging period. A significant characteristic for low temperature charging is that the $E_{(-)}$ cannot recover to 0 V versus Li^+/Li, and that the $E_{(+)}$ is lower than E_{cell} (Fig. 5a–d). This observation may be associated with these two factors: (1) graphite suffers from a high over-potential due to the decrease in ionic conductivity of elec-

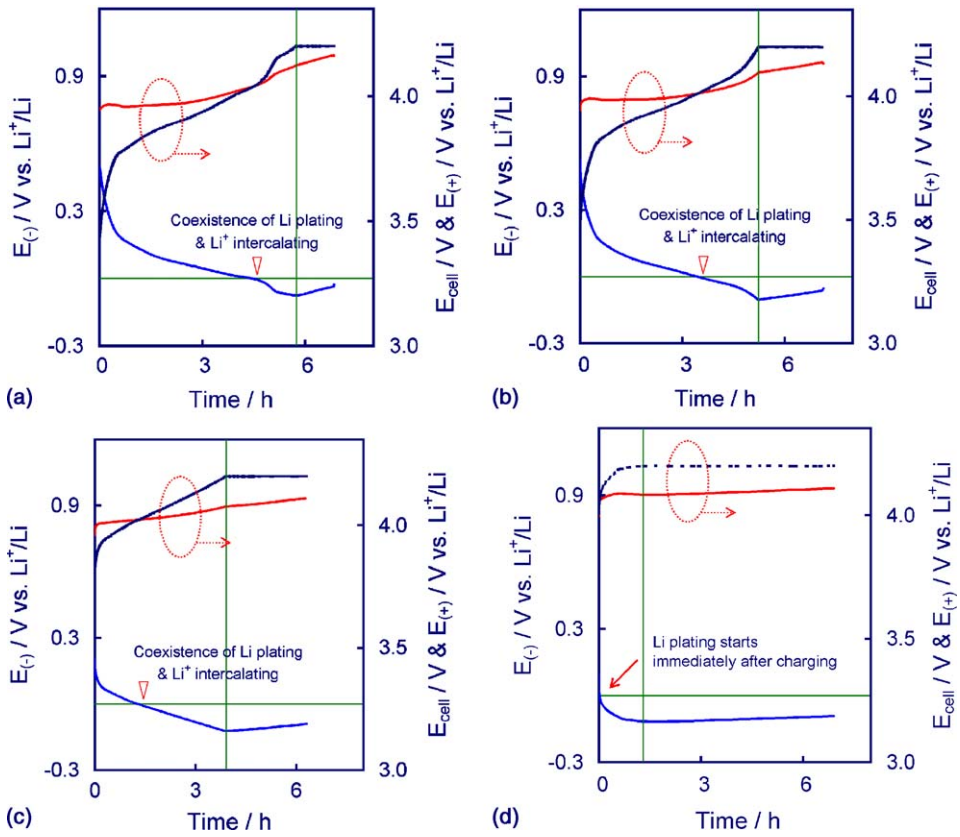

Fig. 5. Correlation of the cell voltage, cathode potential and anode potential with charging time for a 32 mAh MCMB/$LiCoO_2$ cell with a CC of 5 mA at different temperatures: (a) 10 °C, (b) 0 °C, (c) −10 °C and (d) −20 °C.

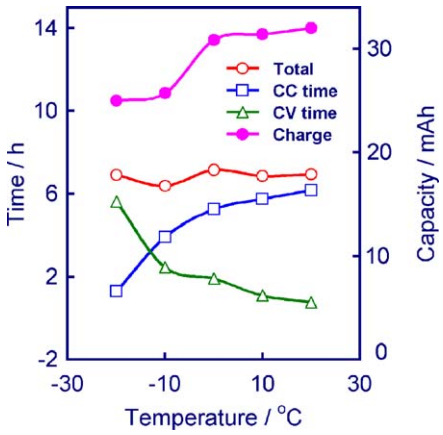

Fig. 6. Effect of cell temperature on the distribution of CC and CV times and on the charging capacity for the MCMB/$LiCoO_2$ cell.

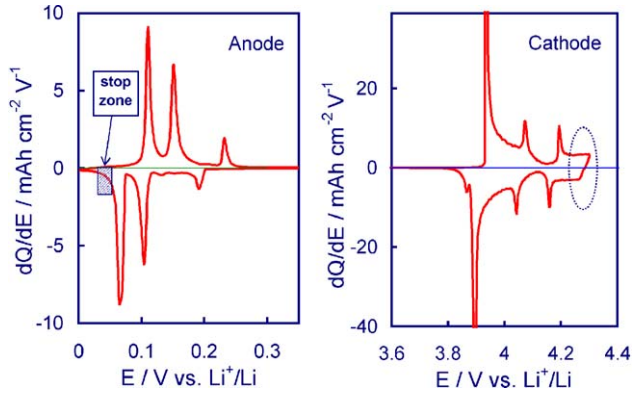

Fig. 7. Plots of differential capacities vs. potential for MCMB and $LiCoO_2$ electrodes, which were recorded during cycling at 0.1*C* using a three-electrode lithium cell, respectively.

trolyte and the slowdown in kinetics of Li^+ ion intercalation into graphite and (2) the plated lithium cannot fully re-intercalate into graphite before the end of charging. The second factor has been confirmed by a slow recovery of the $E_{(-)}$ with the rest time after the charging ends.

Fig. 6 presents the temperature dependence of the charging time and its distribution, which was recorded during charging at 5 mA. As the temperature is at 0 °C or above 0 °C, the charging time is dominated by the CC time, and the charging capacities achieve more than 31 mAh (97% versus the full capacity of 32 mAh). As the temperature drops to −10 °C, the total charging time remains almost unchanged, whereas the portion of the CV time is significantly increased. With respect to the increase of CV time, lithium plating is aggravated and the charging capacity accordingly is decreased from the full capacity (32 mAh) to 26 mAh. These results suggest that Li-ion batteries should not be charged below 0 °C.

3.4. Cell designs for fast charging of a Li-ion cell

The C/A ratio is an essential parameter that affects the cycling performance of Li-ion batteries. In theory, the ideal C/A ratio should be 1.0, that is, the cathode and anode have the same reversible capacities. During charging, a high ratio will result in lithium plating on the anode, while a low ratio will cause overcharge of the cathode, which not only degrades the crystallographic structure of the cathode material but also oxidizes the organic electrolyte solvents. In a real battery system, this ratio should be adjusted in accordance with the properties of the electrode couple. To determine an appropriate C/A ratio for the MCMB and $LiCoO_2$ electrodes, we plotted differential capacities of these two electrodes against the potential in Fig. 7. For the MCMB anode, the lowest lithiation capacity peak potential is 0.065 V versus Li^+/Li. This means that the maximum over-potential for the charging process must not exceed this value, otherwise, Li plating occurs. A good cell design should ensure that the charging process stops in the potential range where the last lithiation capacity peak ends while Li plating does not occur, i.e., in the potential range as marked by a shaded rectangle in Fig. 7. From the capacity–potential plot of the MCMB (Fig. 8), we found that this potential range corresponds to 85–95% capacity of the MCMB. For the $LiCoO_2$ cathode, it is shown that the differential capacities of $LiCoO_2$ cannot decline to 0 at the end of charging, as shown by an ellipse in Fig. 7. This means that additional Li^+ ions will be released from the cathode in the last taper charging period. Based on the above facts, we consider that the more preferable C/A ratio for a MCMB/$LiCoO_2$ Li-ion cell should be 0.85–0.90. This value should be changed with the type of graphite and cathode, which depends on their differential capacity plots versus potential. For example, for $LiMn_2O_4$ and $LiFePO_4$ cathodes whose differential capacity falls to zero at the end of charging, their C/A ratios might be raised to the 0.90–0.95 range. On the other hand, for a cell designed for slow charging, its C/A ratio might be slightly higher since in this case the anode suffers less over-potential so that more capacity can be accessed during the lithiation process.

In the present work, the C/A ratio was determined to be 0.985 by cycling a half-cell (three-electrode) at 0.1*C* between 1.0 and 0.002 V versus Li^+/Li for a Li/MCMB cell and between 2.7 and

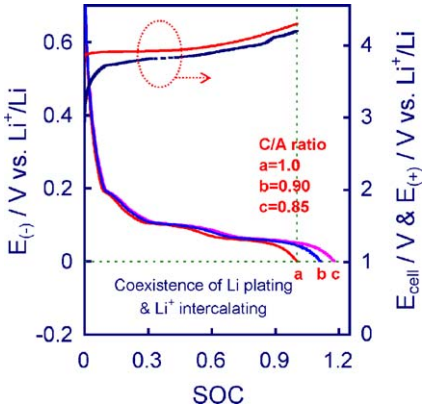

Fig. 8. Correlation of the SOC with E_{cell} (dot line), $E_{(+)}$ (top solid line) and $E_{(-)}$ for the MCMC/$LiCoO_2$ cells with different C/A ratios, which was recorded at *C*/10 from a three-electrode cell. Note that the C/A ratio has negligible influence on the E_{cell} and $E_{(+)}$, therefore, these cells with different C/A ratios share the same E_{cell} and $E_{(+)}$ curves.

4.2 V versus Li^+/Li for a Li/$LiCoO_2$ cell, respectively. This value is rather high compared with the range of 0.85–0.90. This would be the main reason why lithium plating was observed under most of the charging conditions.

4. Conclusions

The results of this work show that lithium plating occurs under most charging conditions, especially at high current rates and at low temperatures. However, the formation of dendritic lithium is effectively suppressed by the subsequent re-intercalation of the plated lithium into graphite. Increasing the current does not reduce the charging time significantly once the current reaches a certain level. Similarly, lowering the temperature does not increase the charging time when the temperature is below 0 °C. Instead, lithium plating is promoted by increasing the current or by lowering the temperature. In these cases, the charging capacities achieved are accordingly decreased. Finally, it should be noted that the conclusions above are based on the specific MCMC–$LiCoO_2$ system and on the $LiBF_4$-based electrolyte. There might be some differences for the other Li-ion chemistries.

References

[1] Y. Nishi, J. Power Sources 100 (2001) 101.
[2] R.F. Nelson, J. Power Sources 107 (2002) 226.
[3] T. Takamura, Solid State Ionics 152–153 (2002) 19.
[4] O. Bitsche, G. Gutmann, J. Power Sources 127 (2004) 8.
[5] S.I. Tobishima, K. Takei, Y. Sakurai, J.I. Yamaki, J. Power Sources 90 (2000) 188.
[6] K. Takamoro, J. Tabuchi, M. Watanabe, Y. Hirota, NEC Res. Develop. 44 (2003) 315.
[7] K. Takeno, M. Ichimura, K. Takano, J. Yamaki, S. Okada, J. Power Sources 128 (2004) 67.
[8] R. Gitzendanner, F. Puglia, C. Martin, D. Carmen, E. Jones, S. Eaves, J. Power Sources 136 (2004) 416.
[9] B. Mammano, Unitrode Power Supply Design Seminar Book, Topic 2, SEM-1000, 1995.
[10] W.F. Bentley, D.K. Heacock, Proceeding of the IEEE 11th Annual Battery Conference on Applications and Advances, Long Beach, CA, January 9–12, 1996, p. 223.
[11] M.J. Isaacson, R.P. Hollandsworth, P.J. Giampaoli, F.A. Linkowsky, A. Salim, V.L. Teofilo, Proceeding of the IEEE 15th Annual Battery Conference on Applications and Advances, Long Beach, CA, January 11–14, 2000, p. 193.
[12] S.S. Zhang, K. Xu, T.R. Jow, Electrochem. Commun. 4 (2002) 928.
[13] S.S. Zhang, K. Xu, T.R. Jow, 205th ECS Meeting Abstracts, No. 82, San Antonio, TX, May 9–14, 2004.